coatings

MDPI

Article

Influence of Remaining Oxide on the Adhesion Strength of Supersonic Particle Deposition TiO_2 Coatings on Annealed Stainless Steel

Noor irinah Omar [1,*], Yusliza Yusuf [1], Syahrul Azwan bin Sundi [1], Ilyani Akmar Abu Bakar [2], Verry Andre Fabiani [3], Toibah Abdul Rahim [4] and Motohiro Yamada [5]

[1] Faculty of Mechanical Engineering and Manufacturing Technology, Universiti Teknikal Malaysia Melaka, Durian Tunggal, Melaka 76100, Malaysia
[2] School of Civil Engineering, College of Engineering, Universiti Teknologi MARA, Shah Alam 40450, Malaysia
[3] Department of Chemistry, Faculty of Engineering, Universitas Bangka Belitung, Pangkalpinang 33172, Indonesia
[4] Faculty of Manufacturing Engineering, Universiti Teknikal Malaysia Melaka, Durian Tunggal, Melaka 76100, Malaysia
[5] Department of Mechanical Engineering, Toyohashi University of Technology, 1-1 Tempaku-Cho, Toyohashi 441-8580, Japan
* Correspondence: nooririnah@utem.edu.my; Tel.: +60-1-2366-1044

Abstract: The cold spray or Supersonic Particle Deposition technique has great potential for producing ceramic nanostructured coatings. This technique operates at a processing temperature that is low enough to preserve the initial feedstock materials' microstructure. Nevertheless, depositing ceramic powders using a cold spray can be challenging because of the materials' brittle nature. The interaction between substrate and particles is significantly influenced by substrate attributes, including hardness, material nature, degree of oxidation and temperature. In this study, the effect of the substrate's remaining oxide composition on the adhesion strength of an agglomerated nano-TiO_2 coating was investigated. The results showed that the coating adhesion strength increased for hard materials such as stainless steel and pure chromium as the annealed substrate temperature also increased from room temperature to 700 °C, indicating thicker oxide on the substrate surface. TiO_2 particles mainly bond with SUS304 substrates through oxide bonding, which results from a chemical reaction involving TiO_2-OH^-. Chromium oxide (Cr_2O_3) is thermodynamically preferred in SUS304 and provides the OH^- component required for the reaction. SUS304 shows a thermodynamic preference for chromium oxide (Cr_2O_3), and this enables Cr_2O_3 to provide the necessary OH^- component for the reaction.

Keywords: supersonic particle deposition; titanium dioxide; adhesion bonding; hard material; stainless steel SUS304; pure chromium

Citation: Omar, N.i.; Yusuf, Y.; Sundi, S.A.b.; Abu Bakar, I.A.; Andre Fabiani, V.; Abdul Rahim, T.; Yamada, M. Influence of Remaining Oxide on the Adhesion Strength of Supersonic Particle Deposition TiO_2 Coatings on Annealed Stainless Steel. *Coatings* **2023**, *13*, 1086. https://doi.org/10.3390/coatings13061086

Academic Editor: Lech Pawlowski

Received: 31 March 2023
Revised: 29 May 2023
Accepted: 29 May 2023
Published: 12 June 2023

1. Introduction

Cold spray is a deposition technique that operates in a solid state without melting the feedstock. High-velocity particles transfer their kinetic energy to the substrate, resulting in localized heat and interfacial deformation [1–3]. This in turn leads to mechanical interlocking and metallurgical bonding [4]. Although the bonding process is not fully understood, optimal temperature, critical velocity and energy levels are needed for effective bonding to take place [5,6]. High strain rate formation and localized heating at the particle-substrate interface result in microscopic protrusions, which can cause metallurgical bonding through material deformation and atomic-level interactions [7,8].

Severe plastic deformation of materials determines interface bonding, resulting in metal-jet formation and adiabatic shear instability (ASI) at the interface [9–12]. The native oxide layer is broken due to the impact of the high-velocity particles, thus creating contact between particles and substrates and resulting in jet formation via ASI [13–15]. As opposed

to the results of Hassani-Gangaraj et al. [16], Grujicic et al. [17] and Assadi et al. [5], presented evidence that contradicted the notion that ASI is not a mandatory factor for adhesion in the cold spray process. In response to the statements made by Assadi et al. [18], Hassani-Gangaraj et al. [19] upheld their simulation-driven study, which indicated that ASI was unnecessary for bonding.

The inadequate adhesion and delamination issues of soft and hard or hard and hard interfaces pose significant challenges to industries. Therefore, comprehending the bonding mechanism helps to address these concerns and benefit the advanced manufacturing sector. There is a significant demand for thick copper coatings on steel (SS316L) plates, which are similar to those of bulk copper and show strong adhesion, particularly for application in Tokamaks' vacuum vessels [20,21]. Singh et al. [7] conducted a study to analyze the bonding process between copper particles and steel substrates (soft-on-hard interface) by modifying substrate conditions and cold spray parameters. Drehmann et al. [22], Wustefled et al. [23] and Dietrich et al. [24] discovered that deformation-induced recrystallization near the particle-substrate interface was responsible for the bonding between aluminum particles and a super-finished monocrystalline sapphire substrate. Metallurgical bonding was facilitated by the development of nanoparticles at the interface, leading to increased adhesion strength between the Al_2O_3 monocrystalline ceramic substrate and the malleable Al particles.

The substrate surface plays a crucial role in achieving strong adhesion in cold-sprayed coatings as it determines the bonding strength between the first layer of TiO_2 particles and the outermost surface. When a metal substrate is used, an active oxide layer with a thickness of several micrometers is formed on the outer surface. Upon contact with the substrate surface, the agglomerated TiO_2 particles disintegrate, leading to particle-substrate contact a few nanometers beneath the oxide layer.

Cold spraying is a common method for creating TiO_2 coatings on metallic objects. Combining a powdered photocatalytic oxide metal with a ductile metal powder allows for plastic deformation upon particle impact. However, the presence of metal oxide particles covering 30–80% of the top surface can hinder the performance of the ceramic TiO_2 coating. Nevertheless, studies have shown that thick, pure agglomerated TiO_2 coatings without additional substances exhibit photocatalytic activity comparable to the raw powder [25]. However, these pure agglomerated coatings have weak interfacial adhesion strength, and the bonding mechanism is not fully understood.

This research aimed to investigate how substrate oxidation levels affect the adhesion of coatings to surfaces. Stainless steel (SUS304) was chosen as the substrate to prevent the development of substrate metal jets caused by particle impact. The study considered factors including substrate oxide thickness, chemical composition, and atomic composition.

2. Equipment and Procedures

2.1. Spray Process

Throughout all coating experiments, the spray parameters used are shown in Table 1 below.

Table 1. Spray parameters.

Cold Spray Machine	De-Laval 24TC Nozzle
Gas carrier	N_2
Operating temperature	500 °C
Operating pressure	3 MPa
Traverse speed	10 mm/s
Spray distance	20 mm
Powder feed rate	3 g/min
Pass number	1

2.2. Materials

Agglomerated TiO_2 powder was used as a feedstock (TAYCA Corporation, Osaka, Japan). It had an anatase crystalline form; its average particle size was 7.55 µm (Figure 1).

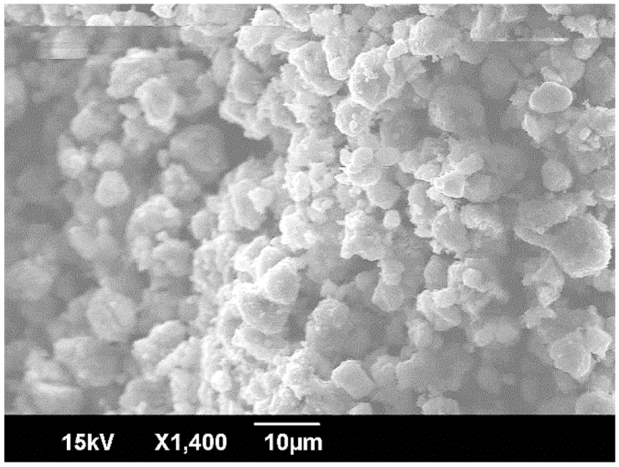

Figure 1. SEM image of Titanium Dioxide powder.

The study utilized two substrates: pure chromium (Cr) and stainless steel (SUS304). To explore the influence of surface oxide at varying temperatures, the substrates were initially subjected to grit-blasting, which was then followed by annealing. The annealing process was conducted under atmospheric conditions using an electric furnace that was set to two different temperatures, specifically 400 °C and 700 °C. The substrates were heated gradually at a rate of 15 °C per 5 min and then soaked for 5 min before being cooled down to room temperature inside the furnace.

2.3. Testings

2.3.1. Testing Tensile-Strength

The study adhered to JIS H 8402 standards and utilized specimens with dimensions of Ø 25 mm × 10 mm to test the adhesion strength. The fracture load value, indicating adhesion strength, was measured using a universal testing machine (Autograph AGS-J, Shimadzu, Kyoto, Japan). For every spraying condition, five specimens were tested, and the average fracture load value was recorded. Furthermore, the fractured coating surface underwent EDX analysis to examine its composition.

2.3.2. Coatings Characterizations

To analyze the TiO_2 coating cross-sectional microstructures on annealed substrates, a scanning electron microscope (SEM: JSM-6390, JEOL, Tokyo, Japan) was employed. A sample measuring 25 mm × 10 mm was embedded in a hardenable resin for observation. The embedded sample underwent a grinding process using silica papers until a #3000 grit size was achieved. Subsequently, it was polished using 1 µm and 0.3 µm alumina suspension.

2.3.3. Micro-Vickers Hardness

The correlation between the adhesion strength of the TiO_2 coating on the annealed substrate and the hardness of the substrate's surface was investigated using a micro-Vickers hardness tester (HMV-G, Shimadzu, Kyoto, Japan). The substrate's hardness was measured with a 98.07 mN test load and a 10 s dwell time applied to the cross-sectional sample. The measurement revealed a hardness value of HV 0.1.

2.3.4. Substrate Oxide Evaluations

The substrate oxide thickness was measured using X-ray photoelectron spectroscopy (XPS) with the ULVAC-PHI Quantera SXM-CI, Kanagawa, Japan. XPS analysis involved using a monochromatic Al Kα source with a current of 15 mA and a voltage of 10 kV. Narrow scans ranging from 0 to 1000 eV were performed for Fe 2p, Cr 2p, and O 1s in order to analyze the different annealed substrates. The measured binding energies were corrected using C 1s at 285.0 eV. Pre-sputtering, which could potentially alter the sample surface and affect the measurements, was not conducted. Detailed XPS analysis conditions for substrate oxide analysis can be found in Table 2.

Table 2. XPS parameter for substrate oxide layer analysis [26].

Regions Measured	Fe 2p, Cr 2p, O 1s
X-ray output	10
Probe diameter	50
Time per step	30
Pass energy	140
Cycle	30

2.3.5. Wipe Test

To investigate the deformation of a single TiO_2 particle on different substrates, a wipe test was performed. Prior to deposition, the substrates were prepared by grinding and polishing to achieve a smooth, mirror-like surface. The spraying process was carried out using nitrogen as the process gas at a temperature of 500 °C and a pressure of 3 MPa. The distance between the nozzle and substrate was maintained at 20 mm, and the process was conducted at a traverse speed of 2000 mm/s. Before spraying, the substrates were cleaned with acetone. The deposition of a single TiO_2 particle on a mirror-polished annealed substrate was observed using the FEI Helios Dual Beam 650 field emission scanning electron microscope (FESEM, FEI, Hilsboro, OR, USA) and focused ion beam (FIB, FEI, Hilsboro, OR, USA) microscope from FEI, based in Oregon, USA.

2.3.6. TEM Testing

To examine the oxide layer post high-velocity cold spraying with various pressures impacting the substrate surface, TEM (transmission electron microscopy) testing was performed. The sample was prepared by creating a thin film, which was then analyzed using field emission gun (FEG) electron microscopy. The analysis was conducted on an EOL JEM-2100F, Tokyo, Japan field emission transmission electron microscope instrument in scanning mode at 200 kV.

3. Result

3.1. Adhesion Strength Testing and Fracture Surface Analysis on Annealed Substrates

Figure 2 illustrates the adhesion strength of TiO_2 coating on pure chromium (Cr) and annealed stainless steel (SUS304). The adhesion strength of both substrates increased as the annealing temperature increased, with values ranging from 0.51 to 2.63 MPa for SUS304 and 0.71 to 1.44 MPa for pure Cr. Figure 3 displays the fracture surface of SUS304 and TiO_2 coating after tensile strength testing, confirming that the fracture occurred at the interface between the substrate and coating and indicating a strong cohesive bond between TiO_2 particles during the coating formation process.

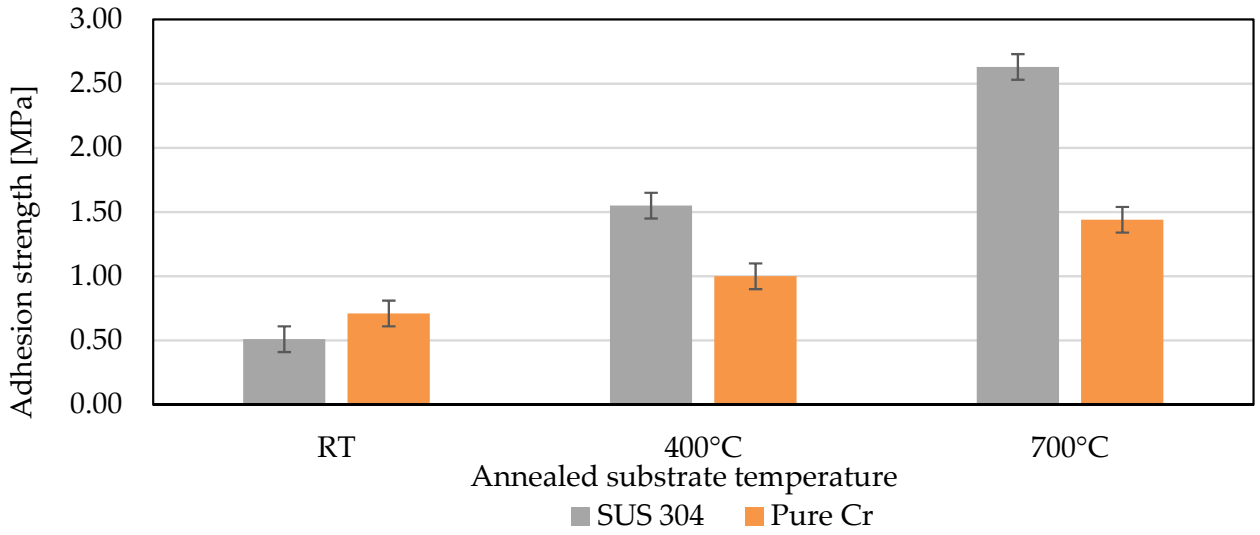

Figure 2. TiO_2 coating adhesion strength on SUS304 and pure Cr from room temperature to 700 °C annealed.

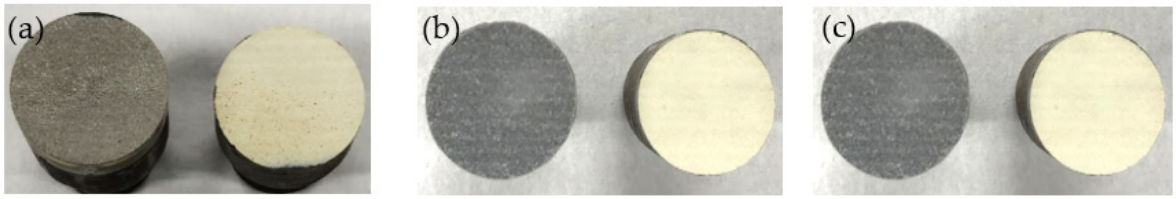

Figure 3. SUS304 fractured surface and TiO_2 coating post tensile strength testing at (**a**) room temperature; (**b**) annealed 400 °C; and (**c**) annealed 700 °C.

Figure 4 depicts the cross-sectional microstructure of SUS304 and TiO_2 coatings at room temperature and 700 °C, representing the conditions with the lowest and highest adhesion strengths, respectively. The coating exhibited a thickness of 200 to 300 µm, indicating the achievement of the critical velocity of particles during the spraying process. Figures 5 and 6 present the results of EDS analysis and the spectrum of the fractured TiO_2 coating on pure chromium substrates annealed at room temperature and 700 °C, respectively. Figure 6 demonstrates a notable presence of chromium in the fractured coating of the substrate annealed at 700 °C compared to the room-temperature substrate. This suggests that chromium oxide may influence the bonding mechanism, potentially contributing to the observed increase in adhesion strength in Figure 2. However, further investigation is required to fully comprehend the role of chromium oxide in the bonding process.

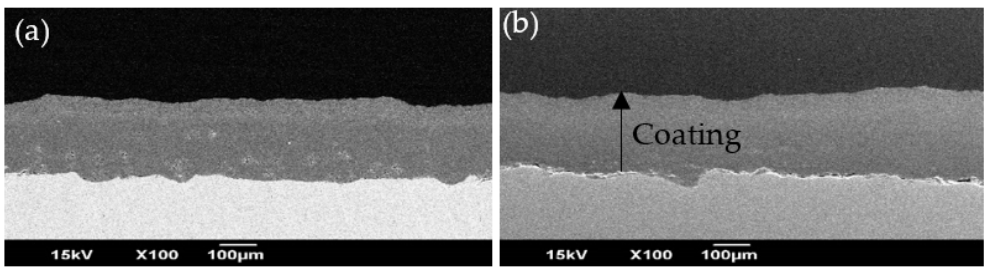

Figure 4. SUS 304 cross-sectional microstructure and TiO_2 coating at (**a**) room temperature; and (**b**) annealed 700 °C.

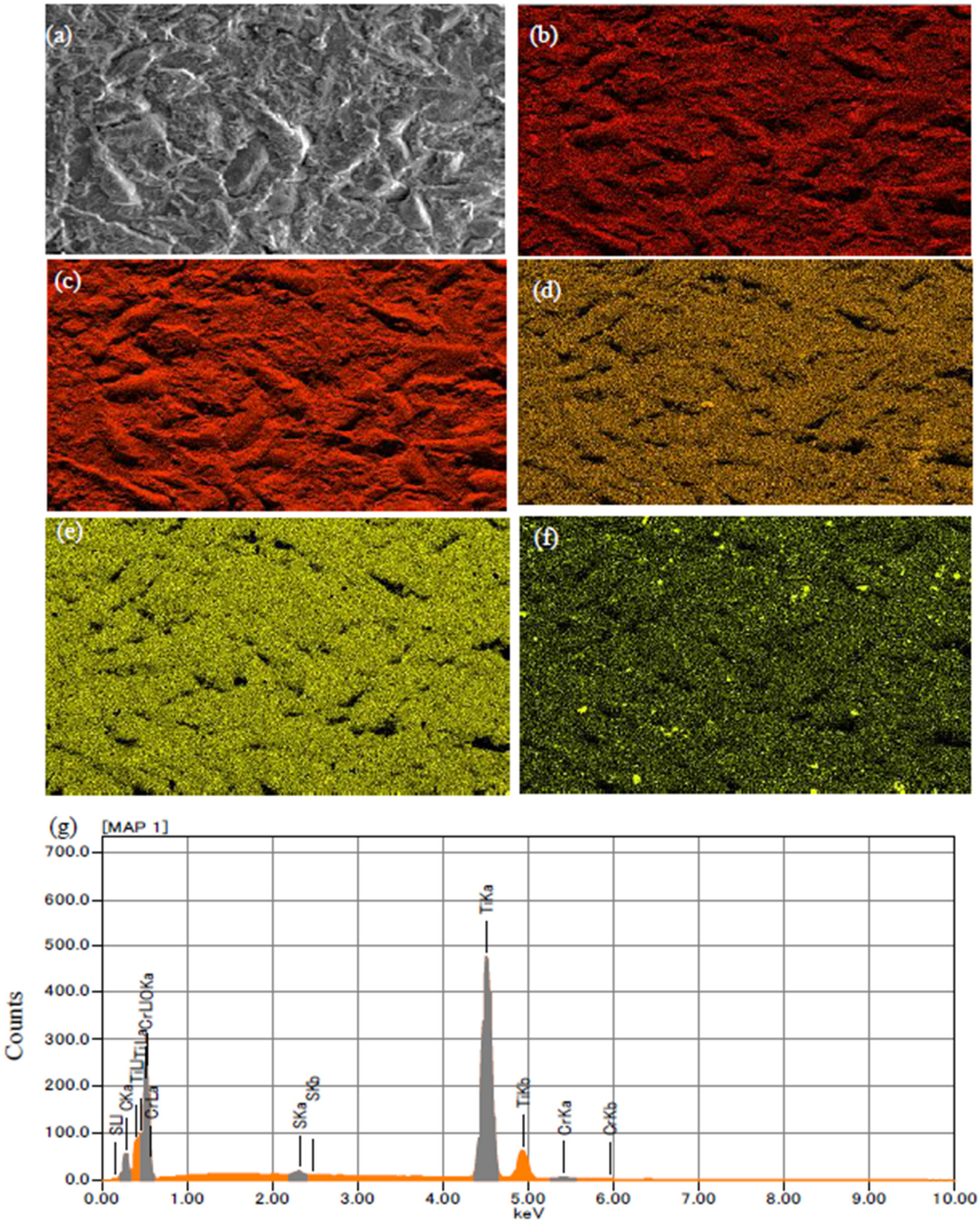

Figure 5. EDX elemental mappings of TiO_2/annealed pure Cr fracture coating: (**a**) SEM; (**b**) carbon; (**c**) oxygen; (**d**) sulfur; (**e**) titanium; (**f**) chromium; (**g**) map sum spectrum for room temperature pure Cr.

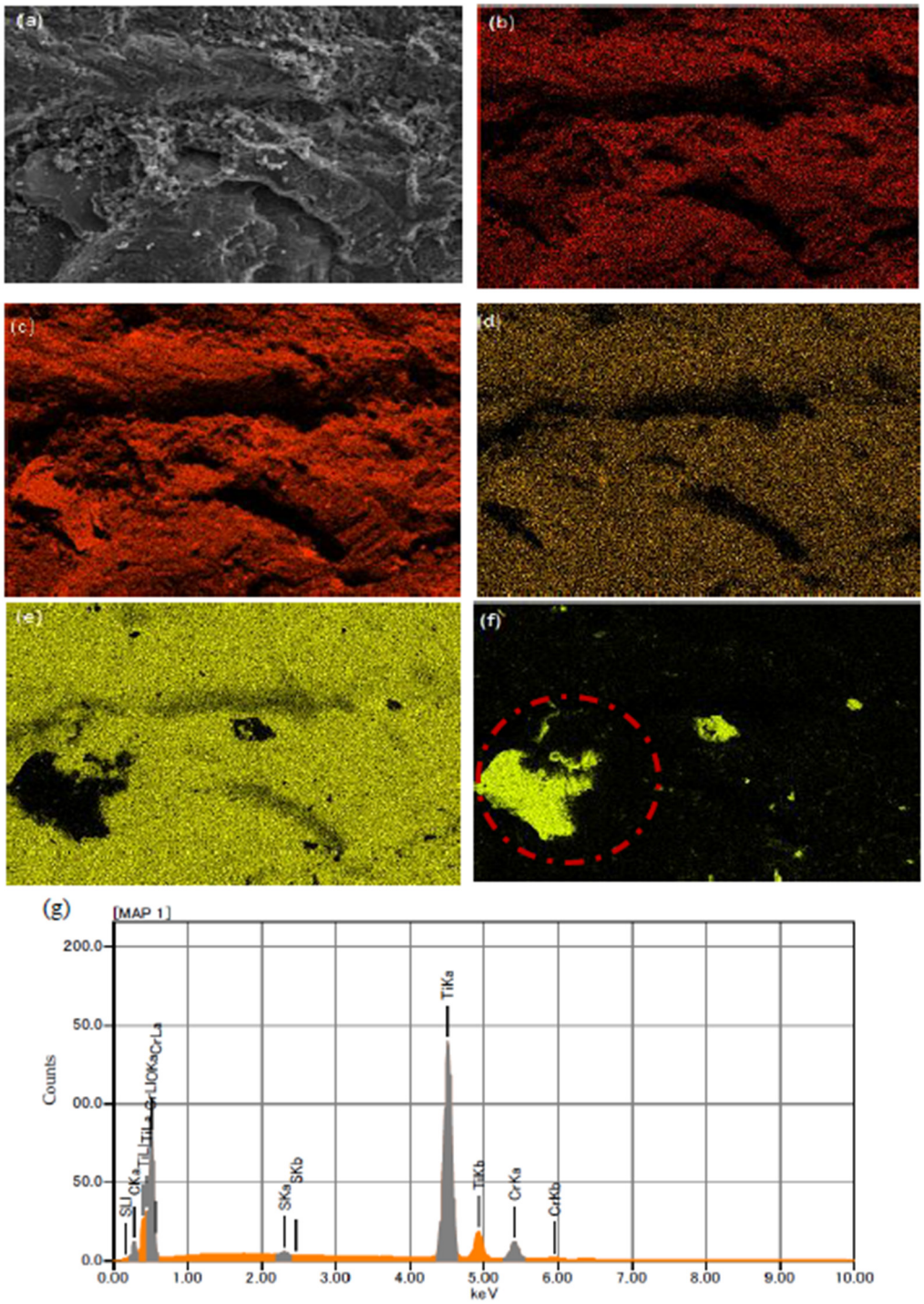

Figure 6. EDX elemental mappings of TiO_2/annealed pure Cr fracture coating: (**a**) SEM; (**b**) carbon; (**c**) oxygen; (**d**) sulfur; (**e**) titanium; (**f**) chromium; (**g**) map sum spectrum for 700 °C annealed pure Cr.

3.2. Depth Profile of Oxide Layer

Variations in the levels of oxygen and chromium within the substrates concerning their depths are illustrated in Figure 7a–c. The results demonstrated that there is a correlation between annealing temperature and the concentration of oxygen within the near-surface area. As the temperature of the substrate increased, the thickness of the pure chromium oxide layer also increased, leading to an increase in the adhesion strength of the TiO_2 coating upon pure chromium annealed substrate from room temperature to 700 °C annealed.

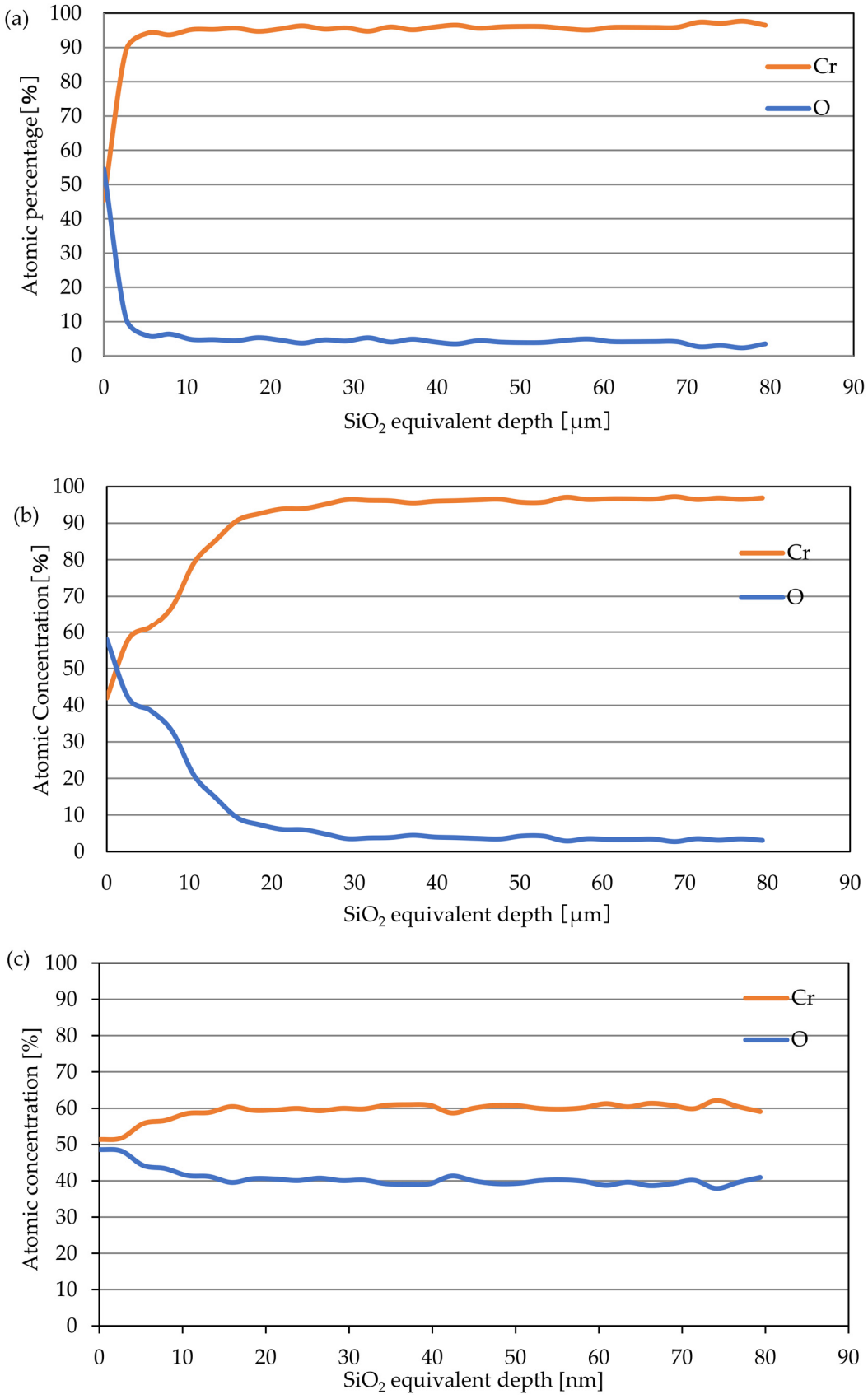

Figure 7. Depth profile analysis of pure Cr (**a**) Room temperature; (**b**) annealed 400 °C; and (**c**) annealed 700 °C.

Additionally, Figure 8a–c, which depicts the analysis of the oxide layer on SUS304, indicated that the thickness of the stainless-steel oxide layer also increased with the annealing temperature of the substrate. According to Ko et al. [27], when Cu/AlN and Al/ZrO_2 bonding couples are formed, the oxide layer becomes amorphous and atomic intermixing occurs at the interface due to chemical adhesion.

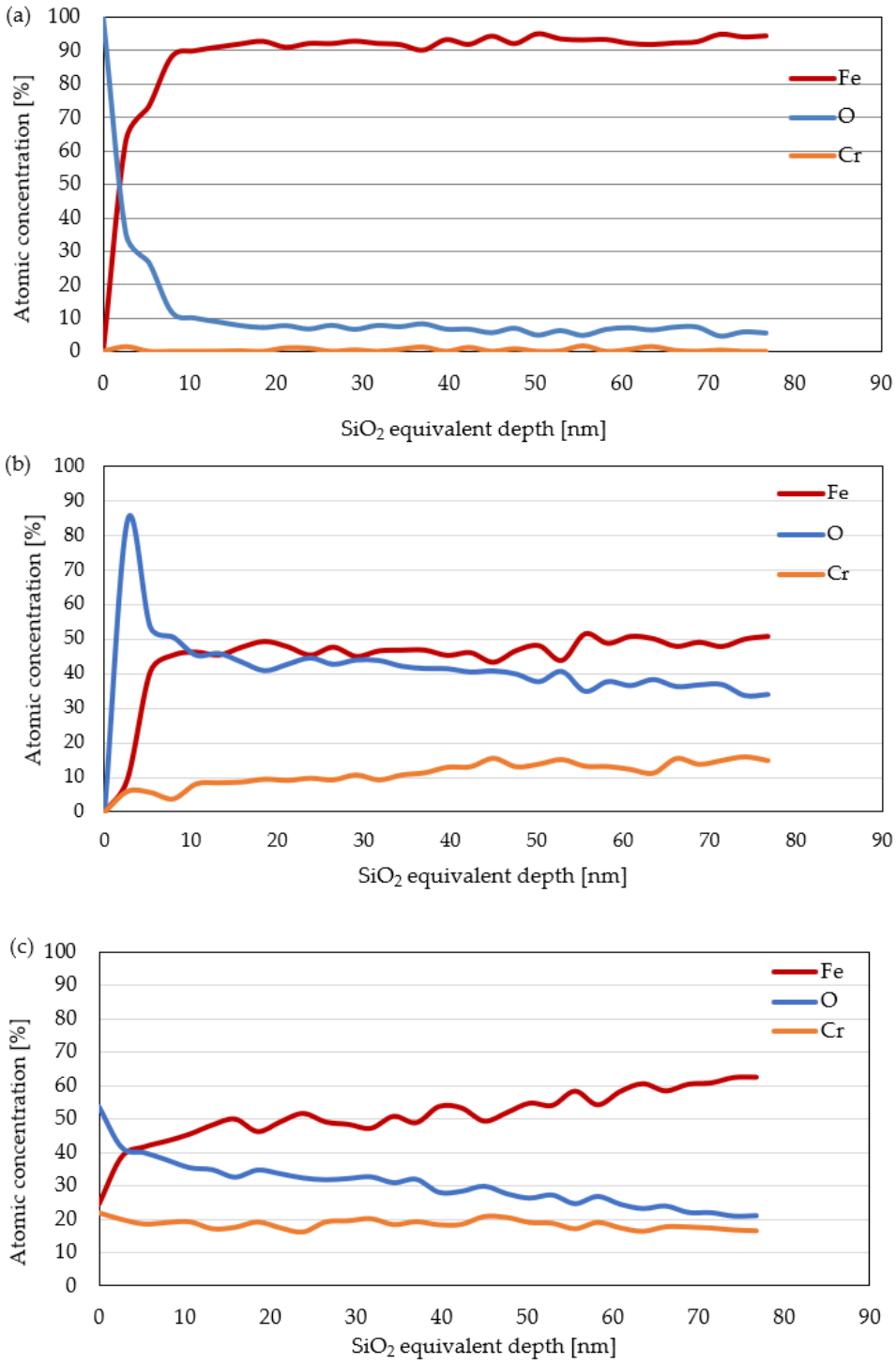

Figure 8. Depth profile analysis of SUS304 at (**a**) Room temperature; (**b**) annealed 400 °C; and (**c**) annealed 700 °C.

The results of this study indicated that the thicker oxide layers on the surface and higher temperatures led to increased adhesion strength of TiO_2 coating upon SUS304 and

pure Cr. The bonding mechanism was influenced by the characteristics of Cr_2O_3 oxide between room temperature and 700 °C. Hence, further research would be conducted on the oxide's chemical composition.

3.3. Evaluation of the Chemical State of Iron, Chromium and Oxygen in the Oxide Layer

Figure 9a,b depict the oxygen content and chemical state of chromium, respectively. Figure 9a shows that the oxide layer on pure chromium at room temperature exhibits a dominant peak for chromium metal at 574.0 eV. In contrast, for pure chromium substrates annealed at 400 and 700 °C, Figure 9a illustrates the presence of a peak at 576.0 eV, corresponding to Cr_2O_3, across the outermost surface of the oxide layer. This indicates that Cr_2O_3 is the primary component of the oxide layer at these annealing temperatures.

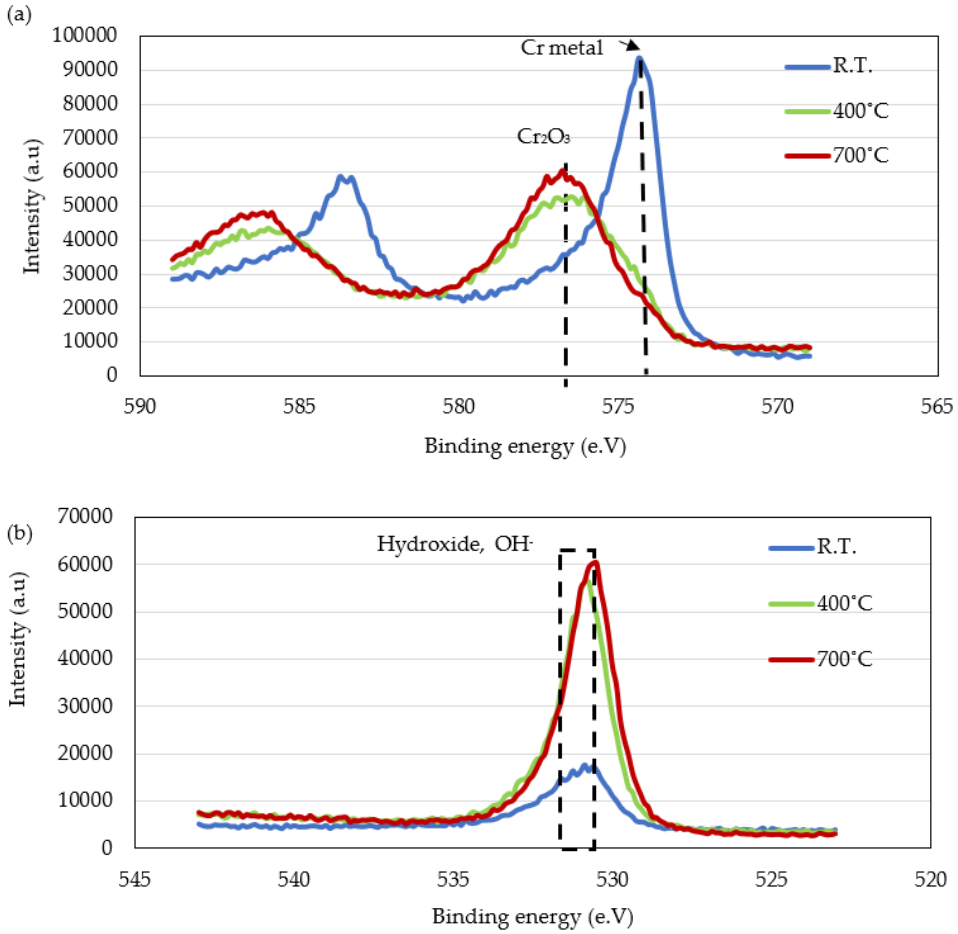

Figure 9. XPS spectra of (**a**) chromium; (**b**) oxygen for annealed pure chromium.

Figure 9b highlights the presence of hydroxide (OH^-) at the outermost surface of the oxide layer for pure chromium substrates annealed from room temperature to 700 °C. The red-dotted line represents a peak position of 531–532 eV, indicating the presence of hydroxide. The study findings suggest that the presence of hydroxide in the oxide layer, ranging from room temperature to 700 °C annealing temperatures, contributes to the observed trend of increasing adhesion strength of the coating with higher annealing temperatures.

Figure 10a–c provides a visual representation of the oxide layer chemical composition in SUS304. The chemical condition of ferum and chromium in SUS304 was identified via the 2P3/2 atomic orbital satellite peak. In Figure 10a, the location of the iron metal peak for stainless steel, which was roughly 706.7 eV [28], was observed on the outer surface of the room-temperature SUS304 substrate (a). When the SUS304 substrate was annealed at 400 °C and 700 °C, the outermost surface of the substrate showed a peak position of hematite Fe_2O_3 (Fe^{2+}) at around 709.3 eV [28]. This result suggested that there was a shift

within the chemical state of the SUS304 substrate from a Fe metal state at room temperature to the hematite state after annealing at 400 °C and 700 °C.

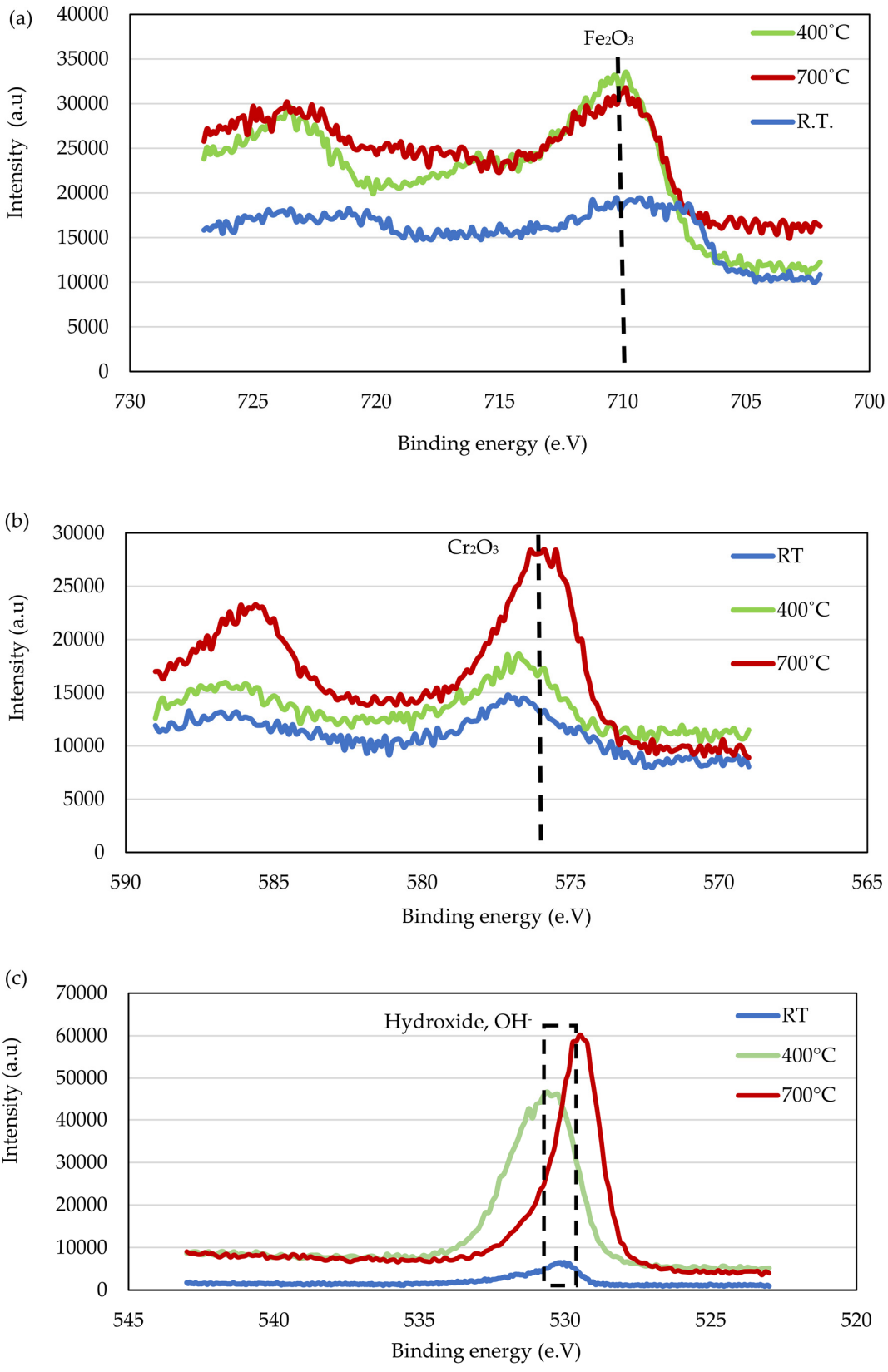

Figure 10. XPS spectra of SUS304: (**a**) Iron; (**b**) Chromium; and (**c**) oxygen.

The oxide layer of SUS304 at room temperature mainly consisted of chromium metal, as indicated by the notable peak at 574.0 eV [29]. For SUS304 substrates annealed at 400 and 700 °C, the peak position of Cr_2O_3 at 576.0 eV was observed across the outer surface of the oxide layer [28], demonstrating a shift from the metal state of chromium to the chromium oxide state. In Figure 10c, the red-dotted line demonstrated the presence of hydroxide, OH^-, between 531 and 532 eV [28], suggesting that the oxide layer for SUS304 at 400 and 700 °C was a combination of Cr_2O_3, Fe_2O_3 and hydroxide.

The process of cold spraying metal particles onto glass or ceramic substrates involves various factors, including the chemical characteristics of the substrates and the impact particles. In a study conducted by Song et al. [30], they examined the cold spraying of Al particles onto a glass substrate. This resulted in the formation of an 80 nm-thick interlayer between the Al particle and the glass substrate. The interlayer exhibited nanocrystalline grains and an amorphous phase, with a notable presence of sodium enrichment. The formation of this interlayer is believed to be a result of the high temperatures generated during the impact process, which induce a reaction between the Al particle and the glass substrate, leading to the formation of liquid stages at the interface.

The strong adhesion observed between the Al particles and the glass substrate is attributed to the high affinity of Al for oxygen within the substrate. The study findings regarding the adhesion strength of coatings on hard metal substrates align with the results reported by Song et al. They conducted a single particle study or wipe test to further investigate the influence of the chemical composition of the oxide layer on the substrate surface on the bonding mechanism.

3.4. Interface Oxide Layer TEM Analysis between TiO_2 Particle at Room Temperature and 700 °C Annealed Substrates

Figure 11 shows high-magnification images that illustrate the presence of an amorphous stage at the interlayer between annealed SUS304 and a single-particle TiO_2. The interlayer thickness was approximately 10 nm, confirming the existence of an interface oxide layer formed after cold-spraying TiO_2 onto SUS304.

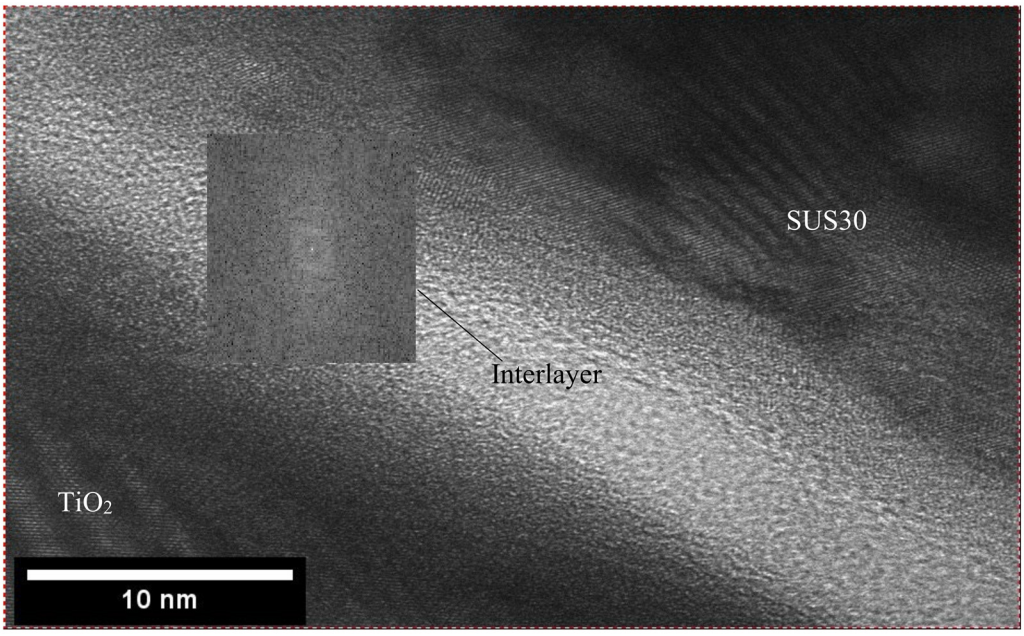

Figure 11. TiO_2/700 °C annealed SUS304 at the interlayer area and FTT image on the oxide layer.

In a study conducted by Kim et al., kinetic spraying was employed to deposit single titanium particles onto mirrored steel substrates. Their findings revealed the presence of a thin amorphous oxide layer at the interface between the particle and the substrate, even after experiencing severe plastic deformation due to particle impacts. This oxide

layer left on the substrate surface after cold spraying acted as a bonding agent between the deposited particle and the substrate [31]. The bonding mechanism involved in this process was further investigated through TEM line analysis, focusing on both the room temperature and 700 °C annealed substrates.

The TEM line analysis shown in Figure 12a,b provided insights into the composition of a single-particle TiO_2 on annealed SUS304 at room temperature and 700 °C. The analysis revealed the presence of Ti, O and Cr atoms. The Ti and O atoms were attributed to the TiO_2 coating and hydroxide on the substrate surface, while the Cr atoms indicated the presence of the oxide layer on SUS304. At room temperature, the substrate exhibited Cr metal along with a combination of $Fe_2O_3^+$, Cr_2O_3 and OH^-. Annealing SUS304 at 700 °C resulted in the highest coating adhesion strength. The presence of Cr_2O_3 oxide may influence the bonding mechanism.

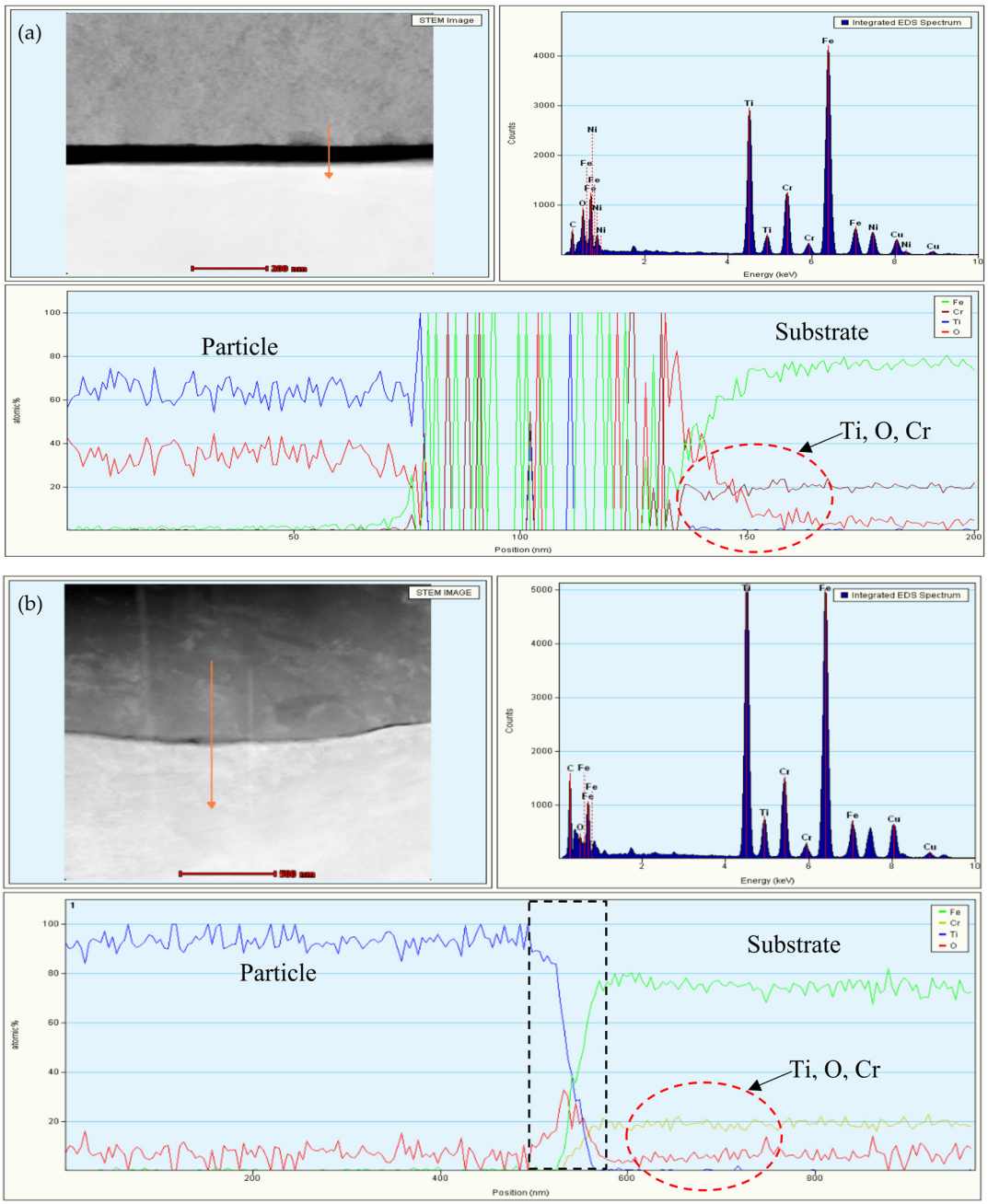

Figure 12. TEM line analysis of the TiO_2 at (**a**) room temperature and (**b**) 700 °C annealed SUS304.

In line with these findings, Song et al. [29] highlighted the importance of considering various factors, including the chemical characteristics of substrates and impact particles, when cold spraying metal particles onto glass or ceramics. Similarly, Drehmann et al. [22] investigated the effect of substrate pre-heating on the adhesion strength of Al particles on an AlN substrate with different levels of softness and hardness. They found that annealing the as-sprayed samples improved the adhesion strength. Increasing the temperature of the AlN substrate before spraying resulted in higher adhesion strength, which was attributed to the thermal energy input that triggered atomic mobility at the Al-AlN interface. Deformation-induced recrystallization near the interface also contributed to atomic mobility, reducing the grain orientation mismatch and improving adhesion strength.

3.5. Oxide Composition Evaluation at Interface of Coating Using X-ray Photoelectron Spectroscopy

Figure 13 provides a schematic diagram of the fracture coating surface on the 700 °C annealed substrate, as analyzed using the XPS method. The purpose of this analysis was to determine the chemical states of the elements present after the cold spray process. Both wide and narrow scan analyses were performed, and the results are presented in Figure 14a–c.

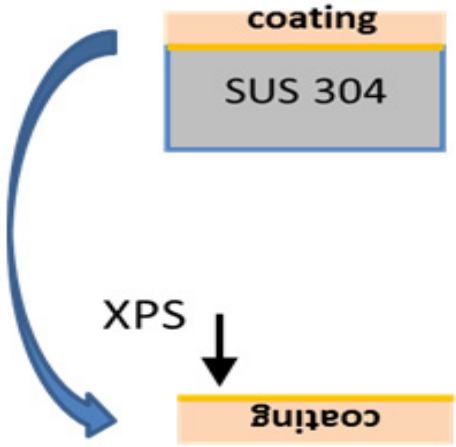

Figure 13. Fracture coating surface at 700 °C annealed.

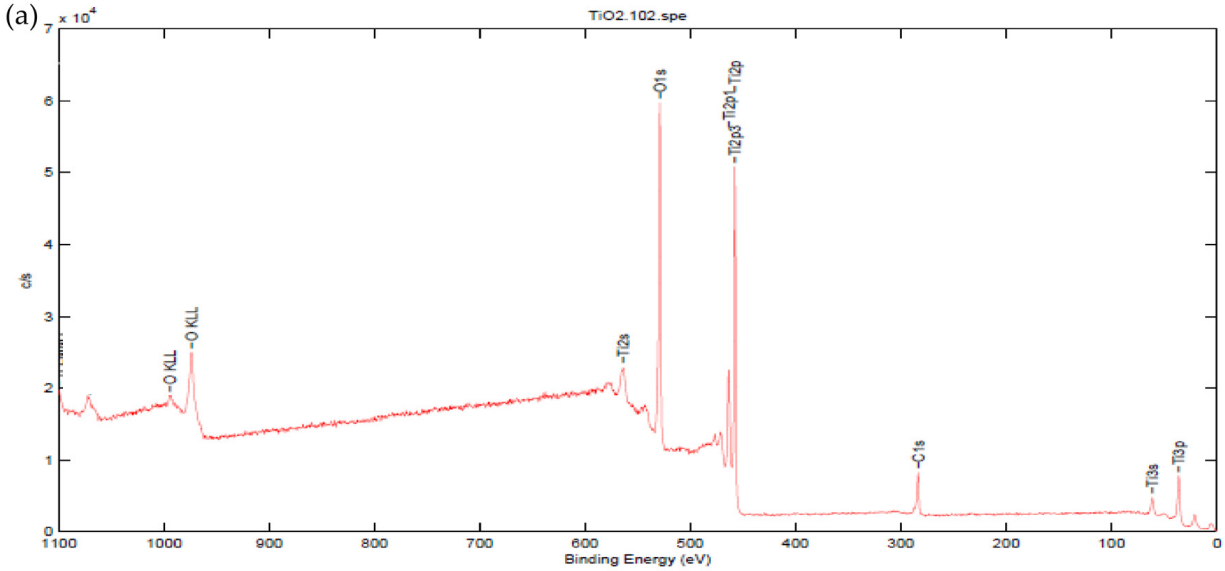

Figure 14. *Cont.*

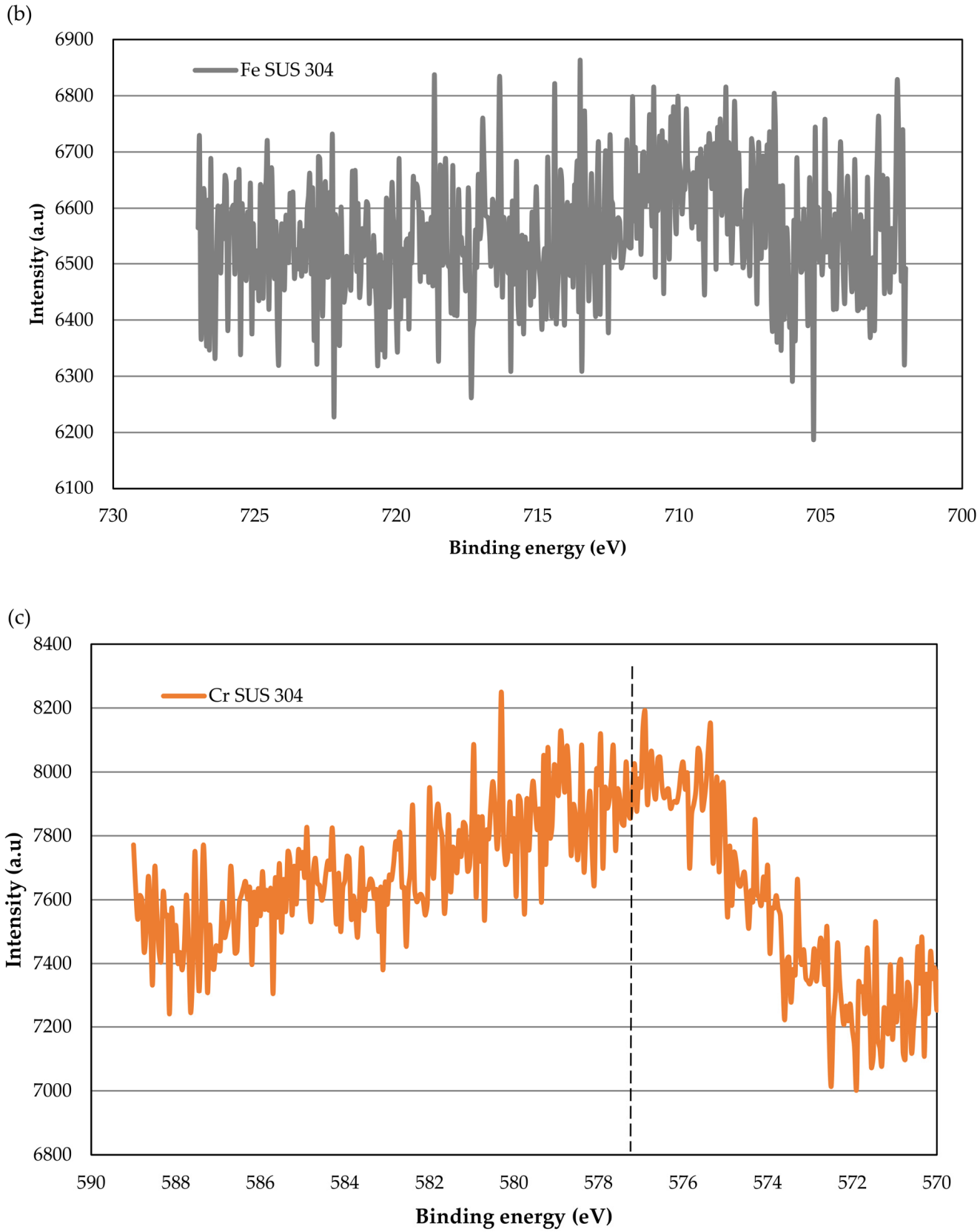

Figure 14. (**a**) Fracture coating interface SUS304 wide scan analysis and narrow scan analysis of coating fracture for (**b**) ferum and (**c**) chromium.

In Figure 14a, the wide-scan analysis of the coating interface reveals the presence of peaks corresponding to titanium, oxygen, carbon, and sodium elements. However, no traces of iron or chromium elements were detected during the wide-scan analysis. Moving to Figure 14b, the narrow analysis of the iron element shows the absence of an elemental peak at the coating interface. Conversely, Figure 14c demonstrates the detection of a chromium elemental peak at a position of 577 eV, indicating the presence of chromium hydroxyls (CrOOH). This suggests that the chemical state of chromium changed from Cr2O3 to CrOOH as a result of the reaction between the chromium oxide (Cr_2O_3) present on the oxide layer of the substrate surface and water molecules in the atmosphere during the cold spray process. It has been confirmed that the oxide layer's thickness increased as the substrate annealing temperature increased, resulting in a thicker layer of Cr_2O_3 on the substrate surface. This, in turn, contributes to the increase in coating adhesion strength. The highest coating adhesion strength was observed at 700 °C annealed substrates, with values of 2.63 MPa for SUS304 and 1.44 MPa for pure Cr. This finding indicates the importance of oxide thickness in influencing the increase in coating adhesion strength for SUS304.

Delamination and weak adhesion strength at interfaces between different materials pose significant challenges in various industries. Understanding the bonding mechanism is crucial to improving adhesion and overcoming these issues. The adhesion strength of cold spray coatings is influenced by factors such as adiabatic shear instability, static recrystallization, mechanical interlocking, and plastic deformation of colliding materials. The state of the substrate plays a significant role in these factors, affecting the bonding properties and characteristics of the cold-sprayed coatings.

In a study conducted by Salim et al. [32], it was found that varying spraying parameters had minimal impact on the adhesion strength of coatings, indicating that mechanical interlocking and substrate shear instability were not the primary bonding mechanisms. Instead, the adhesion strength was influenced by the hardness and oxidizability of the substrates. Modifying the surface chemistry of the substrates could enhance the adhesion strength of TiO_2 coatings. Chemical or physical bonding mechanisms were identified as the primary bonding mechanisms for ceramic coatings, supported by evidence of chemical bonding among TiO_2 particles in TEM images. Additionally, preheating increased the oxidizability of the substrate, which could decrease the adhesion strength of coatings, aligning with the chemical bonding mechanism.

According to Yamada et al., the agglomerated powder of TiO_2 consisted of main particles on the nanoscale with nanoporosity, resulting in a fractured surface with a dangling bond structure. Upon impact, the particles broke apart and then re-bonded, forming a more stable surface and enabling the bonding of newly impacting particles. The formation of the coating involved an interoxide reaction between TiO_2-OH^- and the chromium oxide mixture (Cr_2O_3 + Fe_2O_3 + OH^-) on the top layer of annealed stainless steel. It was observed that the TiO_2 coating on the annealed SUS304 substrate increased in adhesion strength as the annealing temperature increased from room temperature to 700 °C. The adhesion of the impact can be influenced by the passivation layer, including its chemistry, thickness and structure. The impact bonding mechanism between cold-sprayed TiO_2 and SUS304 could be significantly influenced by the thickness of the passivation layer, which might seem unexpected at just 3 nm of growth [33–38].

This observation could be explained by considering the localized deformation of the interface that resulted in bonding, which is shown in the schematic diagram (Figure 15).

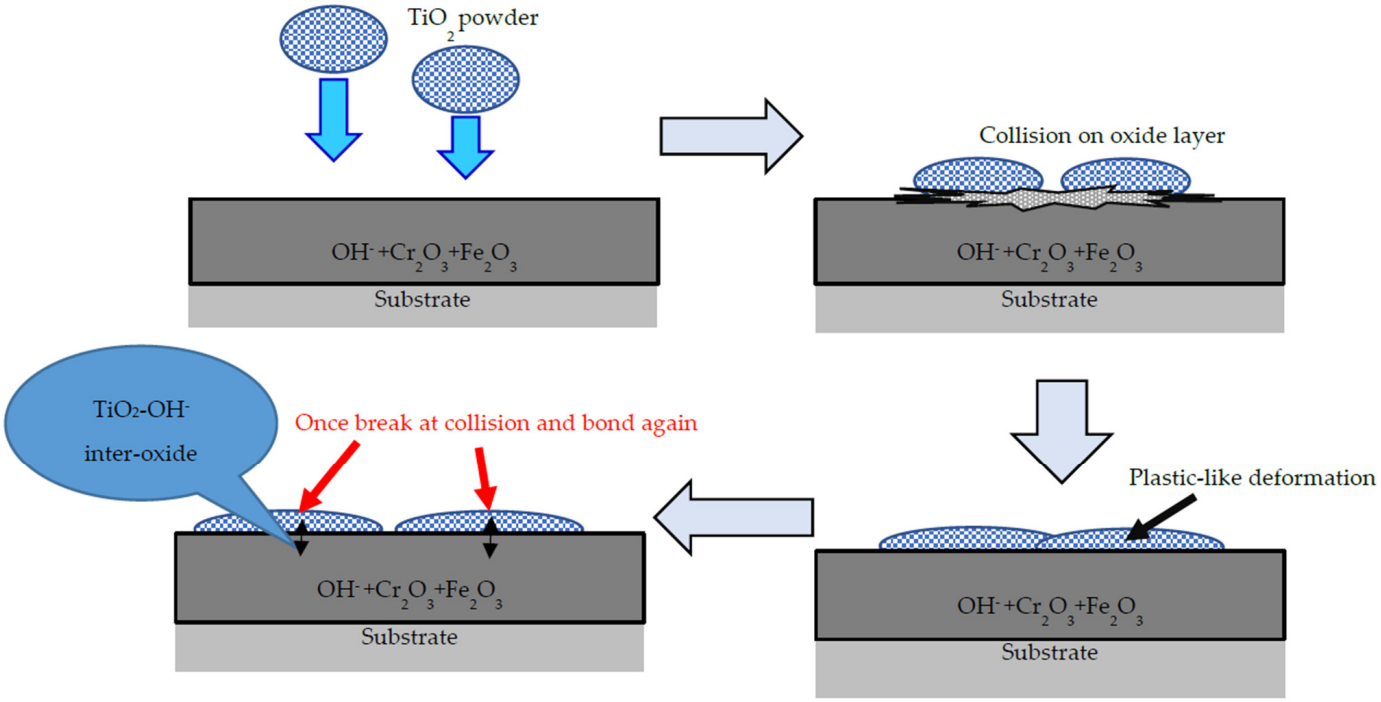

Figure 15. Schematic image of cold-sprayed TiO_2 deposition onto SUS304.

4. Conclusions

In this study, the influence of chromium oxide on the bonding mechanism between pure ceramic titanium dioxide and a SUS304 substrate was investigated. The characteristics of the pure chromium substrate were examined after annealing in an electric furnace at temperatures ranging from room temperature to 700 °C. The key findings can be summarized as follows:

- No detectable traces of iron were found at the coating interface, while a small amount of chromium hydroxyls was observed.
- The chemical state of chromium transformed from Cr_2O_3 to CrOOH due to a reaction between the pre-existing chromium oxide (Cr_2O_3) on the oxide layer of the substrate and water molecules present in the atmosphere during the cold spray process.

Author Contributions: Conceptualization, N.i.O. and M.Y.; methodology, N.i.O.; validation, N.i.O.; formal analysis, N.i.O.; investigation, N.i.O.; resources, N.i.O.; data curation, N.i.O.; writing—original draft preparation, N.i.O.; writing—review and editing, N.i.O., Y.Y., I.A.A.B., V.A.F. and T.A.R.; visualization, N.i.O.; supervision, M.Y.; project administration, N.i.O.; funding acquisition, S.A.b.S. All authors have read and agreed to the published version of the manuscript.

Funding: This research was funded by grant number PJP/2022/FTKMP/S01896.

Institutional Review Board Statement: Not applicable.

Informed Consent Statement: Not applicable.

Data Availability Statement: Not applicable.

Acknowledgments: The study is funded by the Ministry of Higher Education (MOHE) of Malaysia through the short grant (PJP), No: PJP/2022/FTKMP/S01896. The authors also would like to thank the Universiti Teknikal Malaysia Melaka (UTeM) for all the support.

Conflicts of Interest: The authors declare no conflict of interest.

References

1. Schmidt, K.; Assadi, H.; Gärtner, F.; Richter, H.; Stoltenho, T.; Kreye, H. Erratum to: From Particle acceleration to impact and bonding in cold spraying. *J. Therm. Spray Technol.* **2009**, *18*, 1038. [CrossRef]
2. Ziemian, C.W.; Wright, W.J.; Cipoletti, D.E. Influence of impact conditions on feedstock deposition behavior of cold-sprayed Fe-based metallic glass. *J. Therm. Spray Technol.* **2018**, *27*, 843–856. [CrossRef]
3. Vidaller, M.V.; List, A.; Gaertner, F.; Klassen, T.; Dosta, S.; Guilemany, J.M. Single impact bonding of cold sprayed Ti-6Al-4V powders on different substrates. *J. Therm. Spray Technol.* **2015**, *24*, 644–658. [CrossRef]
4. Welk, B.A.; Williams, R.E.A.; Viswanathan, G.B.; Gibson, M.A.; Liaw, P.K.; Fraser, H.L. Nature of the interfaces between the constituent phases in the high entropy alloy CoCrCuFeNiAl. *Ultramicroscopy* **2013**, *134*, 193–199. [CrossRef]
5. Assadi, H.; Kreye, H.; Gärtner, F.; Klassen, T. Cold spraying—A materials perspective. *Acta Mater.* **2016**, *116*, 382–407. [CrossRef]
6. Assadi, H.; Gärtner, F.; Stoltenho, T.; Kreye, H. Bonding mechanism in cold gas spraying. *Acta Mater.* **2003**, *51*, 4379–4394. [CrossRef]
7. Singh, S.; Singh, H.; Chaudhary, S.; Buddu, R.K. Effect of substrate surface roughness on properties of cold-sprayed copper coatings on SS316L steel. *Surf. Coat. Technol.* **2020**, *389*, 125619. [CrossRef]
8. Kumar, S.; Bae, G.; Lee, C. Influence of substrate roughness on bonding mechanism in cold spray. *Surf. Coat. Technol.* **2016**, *304*, 592–605. [CrossRef]
9. Alkhimov, A.P.; Papyrin, A.N.; Vyazemskogo, U.; Kosarev, V.F.; Nesterovich, N.I.; Shushpanov, M.M. Gas-Dynamic Spraying Method for Applying a Coating. U.S. Patent No 5,302,414, 12 April 1994.
10. Irissou, E.; Legoux, J.G.; Ryabinin, A.N.; Jodoin, B.; Moreau, C. Review on Cold Spray Process and Technology: Part I—Intellectual Property. *J. Therm. Spray Technol.* **2008**, *17*, 495–516. [CrossRef]
11. Goldbaum, D.; Poirier, D.; Irissou, E.; Legoux, J.-G.; Moreau, C. Review on cold spray process and technology US patents. In *Modern Cold Spray*; Springer: Cham, Switzerland, 2015; pp. 403–429.
12. Moridi, A.; Hassani-Gangaraj, S.M.; Guagliano, M.; Dao, M. Cold spray coating: Review of material systems and future perspectives. *Surf. Eng.* **2014**, *30*, 369–395. [CrossRef]
13. Hussain, T. Cold spraying of titanium: A review of bonding mechanisms, microstructure and properties. *Key Eng. Mater.* **2012**, *522*, 53–90. [CrossRef]
14. Borchers, C.; Stoltenhoff, T.; Gäartner, F.; Kreye, H.; Assadi, H. Deformation microstructure of cold gas sprayed coatings. *Mater. Res. Soc. Symp. Proc.* **2001**, *674*, 710. [CrossRef]
15. Nikbakht, R.; Seyedein, S.H.; Kheirandish, S.; Assadi, H.; Jodoin, B. Asymmetrical bonding in cold spraying of dissimilar materials. *Appl. Surf. Sci.* **2018**, *444*, 621–632. [CrossRef]
16. Hassani-Gangaraj, M.; Veysset, D.; Champagne, V.K.; Nelson, K.A.; Schuh, C.A. Adiabatic shear instability is not necessary for adhesion in cold spray. *Acta Mater.* **2018**, *158*, 430–439. [CrossRef]
17. Grujicic, M.; Zhao, C.I.; De Rosset, W.S.; Helfritch, D. Analysis of the impact velocity of powder particles in the cold-gas dynamic spray process. *Mater. Sci. Eng. A* **2004**, *368*, 222–230. [CrossRef]
18. Assadi, H.; Gärtner, F.; Klassen, T.; Kreye, H. Comment on "Adiabatic shear instability is not necessary for adhesion in cold spray". *Scr. Mater.* **2019**, *162*, 512–514. [CrossRef]
19. Hassani-Gangaraj, M.; Veysset, D.; Champagne, V.K.; Nelson, K.A.; Schuh, C.A. Response to comment on "Adiabatic shear instability is not necessary for adhesion in cold spray". *Scr. Mater.* **2019**, *162*, 515–519. [CrossRef]
20. Singh, S.; Kumar, M.; Sodhi, G.P.S.; Buddu, R.K.; Singh, H. Development of thick copper claddings on SS316L steel for in-vessel components of fusion reactors and copper-cast iron canisters. *Fusion Eng. Des.* **2018**, *128*, 126–137. [CrossRef]
21. Drehmann, R.; Grund, T.; Lampke, T.; Wielage, B.; Manygoats, K.; Schucknecht, T.; Rafaja, D. Splat formation and adhesion mechanisms of cold gas-sprayed Al coatings on Al_2O_3 substrates. *J. Therm. Spray Technol.* **2014**, *23*, 68–75. [CrossRef]
22. Wüstefeld, C.; Rafaja, D.; Motylenko, M.; Ullrich, C.; Drehmann, R.; Grund, T.; Lampke, T.; Wielage, B. Local heteroepitaxy as an adhesion mechanism in aluminium coatings cold gas sprayed on AlN substrates. *Acta Mater.* **2017**, *128*, 418–427. [CrossRef]
23. Dietrich, D.; Wielage, B.; Lampke, T.; Grund, T.; Kümme, S. Evolution of microstructure of cold-spray aluminum coatings on Al_2O_3 substrates. *Adv. Eng. Mater.* **2011**, *14*, 275–278. [CrossRef]
24. Yamada, m.; Isago, H.; Shima, K.; Nakano, H.; Fukumoto, M. Deposition of TiO_2 Ceramic Particles on Cold Spray Process. In Proceedings of the International Thermal Spray Conference & Exposition Raffles City Convention Centre, Singapore, 3–5 May 2010; Marple, G.M.B.R., Agarwal, A., Hyland, M.M., Lau, Y.-C., Li, C.-J., Lima, R.S., Eds.; ASM Thermal Spray Society: Singapore, 2010; pp. 172–176.
25. Moulder, J.F.; Stickle, W.F.; Sobol, P.E.; Bomben, K.D.; Chastain, J. *Handbook of X-ray Photoelectron Spectroscopy*; Perkin-Elmer Corporation Physical Electronics Division: Eden Prairie, MI, USA, 1993; p. 45.
26. Ko, K.H.; Choi, J.O.; Lee, H. The interfacial restructuring to amorphous: A new adhesion mechanism of cold-sprayed coatings. *Mater. Lett.* **2016**, *175*, 13–15. [CrossRef]
27. Mark, C.B. Advanced analysis of copper X-ray photoelectron spectra. *Surf. Interface Anal.* **2017**, *49*, 1325–1334.
28. Goodwin, H.B.; Gilbert, E.A.; Schwartz, C.M.; Greenidge, C.T. A preliminary study of the ductility of chromium. *J. Electrochem. Soc.* **1953**, *100*, 152–160. [CrossRef]
29. Minghui, S.; Hiroshi, A.; Seiji, K.; Kazuhiko, S. Reaction layer at the interface between aluminium particles and a glass substrate formed by cold spray. *J. Phys. D Appl. Phys.* **2013**, *46*, 195301.

30. Christoulis, D.K.; Guetta, S.; Guipont, V.; Jeandin, M. The influence of the substrate on the deposition of cold-sprayed titanium: An experimental and numerical study. *J. Therm. Spray Technol.* **2011**, *20*, 523–533. [CrossRef]
31. Arabgol, Z.; Vidaller, M.V.; Assadi, H.; Gärtner, F.; Klassen, T. Influence of thermal properties and temperature of substrate on the quality of cold-sprayed deposits. *Acta Mater.* **2017**, *127*, 287–301. [CrossRef]
32. Salim, N.T.; Yamada, M.; Nakano, H.; Shima, K.; Isago, H.; Fukumoto, M. The effect of post-treatments on the powder morphology of titanium dioxide (TiO_2) powders synthesized for cold spray. *Surf. Coat. Technol.* **2011**, *206*, 366–371. [CrossRef]
33. Ichikawa, Y.; Ogawa, K. Effect of substrate surface oxide film thickness on deposition behavior and deposition efficiency in the cold spray process. *J. Therm. Spray Technol.* **2015**, *24*, 1269–1276. [CrossRef]
34. Fukumoto, M.; Wada, H.; Tanabe, K.; Yamada, M.; Yamaguchi, E.; Niwa, A.; Sugimoto, M.; Izawa, M. Effect of substrate temperature on deposition behavior of copper particles on substrate surfaces in the cold spray process. *J. Therm. Spray Technol.* **2007**, *16*, 643–650. [CrossRef]
35. Noor irinah, O.; Yamada, M.; Yasui, T.; Fukumoto, M. On the role of substrate temperature into bonding mechanism of cold sprayed titanium dioxide. *IOP Conf. Ser.* **2020**, *920*, 012009. [CrossRef]
36. Viscusi, A.; Astarita, A.; Della Gatta, R.; Rubino, F. A Perspective review on the bonding mechanisms in cold gas dynamic spray. *Surf. Eng.* **2019**, *35*, 743–771. [CrossRef]
37. Dong, S.; Liao, H. Substrate pre-treatment by dry-ice blasting and cold spraying of titanium. *Surf. Eng.* **2018**, *34*, 1173–1180. [CrossRef]
38. Noor irinah, O.; Suhana, M.; Yusliza, Y.; Toibah, A.R.; Zaleha, M.; Syahriza, I.; Ilyani Akmar, A.B.; Santirraprahkash, S. A Preliminary study into the effect of oxide chemistry on the bonding mechanism of cold-sprayed titanium dioxide coatings on SUS316 stainless steel substrate. *J. Electrochem. Sci. Eng.* **2022**, *12*, 579–591.